Article

Surface Wave Propagation in a Rotating Doubly Coated Nonhomogeneous Half Space with Application

Ali M. Mubaraki [1], Maha M. Helmi [1] and Rahmatullah Ibrahim Nuruddeen [2,*]

[1] Department of Mathematics and Statistics, College of Science, Taif University,
P.O. Box 11099, Taif 21944, Saudi Arabia; alimobarki@tu.edu.sa (A.M.M.); m.hlmi@tu.edu.sa (M.M.H.)

[2] Department of Mathematics, Faculty of Science, Federal University Dutse,
Dutse P.O. Box 7156, Jigawa State, Nigeria

[*] Correspondence: rahmatullah.n@fud.edu.ng

Abstract: The current study examines the propagation of surface waves in an asymmetric rotating doubly coated nonhomogeneous half space. The coating layers are assumed to be made of different homogeneous isotropic materials, while the overlaying nonhomogeneous half space layer is considered to be of exponentially varying material properties. The consequential exact vibrational displacements and dispersion relation are determined analytically, in addition to the approximate validation of the dispersion relation via the application of an asymptotic procedure within the long wave limit. Two cases of unloaded and loaded end surface scenarios are analyzed by examining the posed fundamental modes. More precisely, an elastic Winkler foundation was considered in the case of a mechanically loaded end surface condition and was found to proliferate the transition between having a fundamental mode over the frequency axis to the wave number axis as the angular velocity increased. Moreover, the rotational effect was found to have a direct impact on the surface wave propagation with a long wave and low frequency. Aside from that, an increase in the nonhomogeneity parameter resulted in propagation with a relatively long frequency.

Keywords: surface waves; multiple coating; layered media; dispersion relation; anti-plane dynamic

1. Introduction

The propagation of surface waves in various structural configurations has been a topic of much concern in different areas of real-life applications, such as geology, aerospace, seismology, mechanical and civil engineering, and non-destructive analysis, among others [1–5]. Thus, with recent technological advancements, considerable attention has been invested by many scientists in the examination and analysis of the propagation of waves in multilayered elastic structures [6–9]. One could see different studies on the propagation of surface waves, which are mainly governed by Rayleigh waves, Stoneley waves, and Love waves in diverse elastic media (see [10–12] and the references therein). The mechanic of multilayered and coated media has, therefore, been progressively gaining ground in recent times, with the emergence of different layered media and composites, including, for example, metamaterials, nanomaterials, and high-contrast materials to mention a few [13–15]. In particular, there exists an extensive study on the propagation of surface waves on sandwich structures comprising, for instance, the symmetric and asymmetric three- and five-layered laminates [16–20]. In these studies, the asymptotic analysis method was basically considered for the analysis of the resulting dispersion relations among the presence of material contrasts. Moreover, structural symmetry allows dual analysis of the involved fields, as well as the resulting dispersion relation. In essence, an asymptotic approach of study allows an optimized form of propagation within the long-wave low-frequency range [21]. This form of propagation of waves in elastic media is only achievable via the asymptotic analysis methodology.

Furthermore, we digress a little to the dynamics of coated structures [22–24]. Coated structures are equally in higher demand industrially and in day-to-day human life. Accord-

ingly, the propagation of surface waves in a coated media has attracted much concern in engineering, with vast applications including improving highway and rail transportation quality and seismic protection, among others [25–28]. Yet, another area of the relevance of the coated media is in the construction of biomedical devices, where coatings are utilized to reduce the effect of mechanical loads on the surface of implants (for instance, see [29,30]). We must mention here the recent study on the influence of magnetic and gravitational fields on the propagation of surface waves on a coated viscoelastic half-space in a rotating reference [31]. We also recall the recent work on the propagation of Rayleigh waves on a mechanically loaded compressible half space [32]. The effects of surface stresses were examined, in addition to the consequences of the presence of gravity. More related studies can be found in the various related literature, including [33] and the references therein. We also bear in mind certain important references that take into account the significance of material nonhomogeneity with regard to linearly and exponentially varying material constants [34,35] sequentially.

However, the current manuscript examines the propagation of surface waves in an asymmetric rotating doubly coated nonhomogeneous half space via the application of analytical and asymptotic approximation methods. The two coating layers comprising upper and lower coatings are considered to be of different homogeneous isotropic materials, while the overlying nonhomogeneous half space layer is assumed to be of exponentially varying material constants. Two cases of unloaded and loaded mechanical end surface scenarios will be analyzed on the face of the upper coating by examining the resultant dispersion relation through the posed harmonic waves (precisely, the fundamental mode). Moreover, the effects of the nonhomogeneity parameter, elastic Winkler foundation parameter, and the rotational effects on the propagation of surface waves in the governing structure will be analyzed. This paper is organized in the following manner. Section 2 gives the statement of the problem. Section 3 determines the exact expressions for the respective vibrational displacements, while Section 4 acquires the exact expressions for the related dispersion relations. Section 5 presents approximations of the exact dispersion relations, while Section 6 gives a numerical application and discussion of the results. Finally, Section 7 concludes the findings of the study.

2. Statement of the Problem

Consider the asymmetric doubly coated nonhomogeneous half space shown in Figure 1. To be precise, two isotropic coating layers are considered, with the upper coating layer having a constant thickness of h_1 and occupying the region $0 \leq x_2 \leq h_1$, while the lower coating layer has a thickness of h_2 and lies over the region $h_1 \leq x_2 \leq h_1 + h_2$. In addition, the nonhomogeneous half space layer occupies the semi-infinite interval $h_1 + h_2 \leq x_2 < \infty$, and perfect bounding conditions are assumed on the two interfaces (i.e., at $x_2 = h_1$ and at $x_2 = h_1 + h_2$). Importantly, the governing equation of motion is considered to be in the sense of an anti-plane shear propagation [19,20] in favor of its relative simplicity yet models real-life applications perfectly [36,37].

Equations of Motions in the Coating

The anti-plane shear equations of motion in the coating layers in the presence of rotation are given as follows [19,20]:

$$\frac{\partial \tau_{23}^c}{\partial x_2} + \frac{\partial \tau_{13}^c}{\partial x_1} = \rho_c \left(\frac{\partial^2 v_c}{\partial t^2} - \Omega^2 v_c \right), \qquad c = 1, 2, \tag{1}$$

for

$$(x_1, x_2, t) \in R_1 := \{(x_1, x_2, t) : x_1 \in (-\infty, \infty), \ x_2 \in (0, h_1) \cup (h_1, h_1 + h_2), \ t \in (0, T], \}$$

where $c = 1$ and $c = 2$ stand for the upper and lower coatings, respectively, Ω is the angular velocity, ρ_c denotes the densities in the coatings, $v_c = v_c(x_1, x_2, t)$ represents

the displacements, and τ_{m3}^c for $m = 1, 2$ are the respective stresses in the coatings, and defined as

$$\tau_{m3}^c = \mu_c \frac{\partial v_c}{\partial x_m}, \qquad m = 1, 2, \qquad c = 1, 2, \tag{2}$$

where μ_c for $c = 1, 2$ are constant Lame's material constants in the respective upper and lower coating layers.
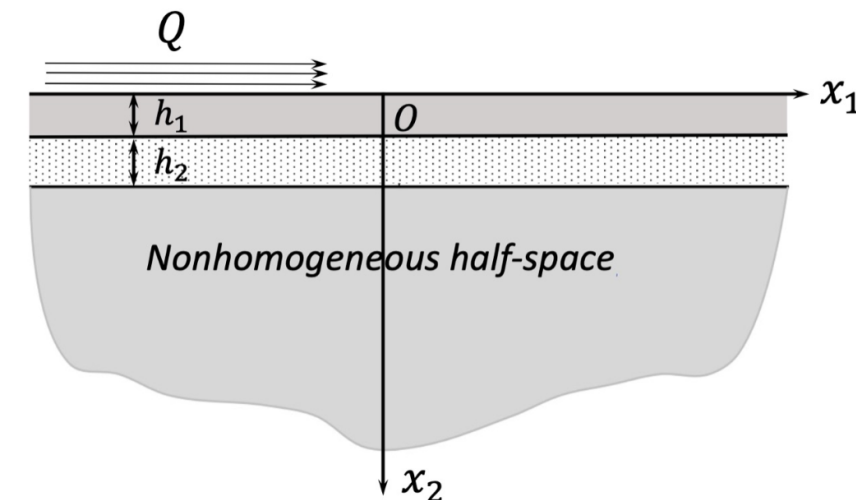

Figure 1. Doubly coated nonhomogeneous half space with tangential load Q.

Equation of Motion in the Nonhomogeneous Half Space

In a similar way, the anti-plane shear equation of motion in the nonhomogeneous half space in the presence of rotation takes the following form:

$$\frac{\partial \tau_{23}^3}{\partial x_2} + \frac{\partial \tau_{13}^3}{\partial x_1} = \bar{\rho}_3(x_2) \left(\frac{\partial^2 v_3}{\partial t^2} - \Omega^2 v_3 \right), \tag{3}$$

for

$$(x_1, x_2, t) \in R_2 := \{(x_1, x_2, t) : x_1 \in (-\infty, \infty), \ x_2 \in (0, \infty), \ t \in (0, T]\},$$

where Ω is the angular velocity, $\bar{\rho}_3(x_2)$ denotes an x_2-dependent density in the nonhomogenous half space, $v_3 = v_3(x_1, x_2, t)$ is the displacement, and τ_{m3}^3 for $m = 1, 2$ are the stresses given by

$$\tau_{m3}^3 = \bar{\mu}_3(x_2) \frac{\partial v_3}{\partial x_m}, \quad m = 1, 2. \tag{4}$$

where $\bar{\mu}_3(x_2)$ is the x_2-dependent Lame's material constant in the nonhomogeneous half space layer. Additionally, as the layer is nonhomogeneous, the material nonhomogeneity with regard to the density $\bar{\rho}_3(x_2)$ and the Lame's material constant $\bar{\mu}_3(x_2)$ are further assumed to be of the following exponential forms [35,38–40]:

$$\bar{\mu}_3(x_2) = \mu_3 \, e^{\beta x_2}, \qquad \bar{\rho}_3(x_2) = \rho_3 \, e^{\beta x_2}, \tag{5}$$

where μ_3 is a Lame's material constant and ρ_3 is a constant density, while β is the dimensional nonhomogeneity parameter. Moreover, the literature is full of various forms of material nonhomogeneities, including, for instance, the linear form [34], quadratic form in [41], and the linear, quadratic, and exponential forms in [42] and in the respective references therein.

Finally, as the present study seeks to comparatively examine the resulting exact and approximate vibrational displacements and dispersion relations, we therefore seek to obtain strong solutions layer-wise. In light of this, it is expected that

$$\{v^c(x_1, x_2, t), v_{x_1 x_1}^c(., x_2, t), v_{x_2 x_2}^c(x_1, ., t), v_{tt}^c(x_1, x_2, .)\} \in C(R_1), \ \text{for} \ c = 1, 2,$$

and

$$\{v^3(x_1, x_2, t), v^3_{x_1 x_1}(., x_2, t), v^3_{x_2 x_2}(x_1, ., t), v^3_{tt}(x_1, x_2, .)\} \in C(R_2),$$

where R_j, for $j = 1, 2$ are defined below Equations (1) and (3), respectively, and $C(R_j)$ are the spaces of continuous functions, where $C(R_j) \subset L^2(R_j,)$ are the Lebesgue square integrable functions.

Boundary Condition

On the end surface of the entire structure $x_2 = 0$, we consider two different boundary conditions:

Case (a): the unloaded end surface (traction-free) condition:

$$\tau^1_{23}(x_1, x_2, t) = 0, \quad \text{at} \quad x_2 = 0, \quad (x_1, t) \in D := \{(x_1, t) : x_1 \in (-\infty, \infty), \ t \in [0, T]\}, \quad (6)$$

Case (b): the loaded end surface (mechanical loading) condition

$$\tau^1_{23}(x_1, x_2, t) = -Q, \quad \text{at} \quad x_2 = 0, \quad (x_1, t) \in D := \{(x_1, t) : x_1 \in (-\infty, \infty), \ t \in [0, T]\}, \quad (7)$$

where Q in the last equation is a mechanical load that is considered to be due to an elastic Winkler foundation, which is expressed as [43]

$$Q = p \, v_1, \tag{8}$$

where p is the dimensional stiffness of the elastic Winkler foundation, while v_1 is the vibrational displacement of the upper coating the load is being excited upon.

Interfacial Conditions

We equally prescribe sufficient perfect interfacial conditions between the upper and lower coating layers $x_2 = h_1$ and between the lower coating layer and the nonhomogeneous half space $x_2 = h_1 + h_2$, respectively, as follows:

$$v_1(x_1, x_2, t) = v_2(x_1, x_2, t), \quad \text{at } x_2 = h_1, \quad (x_1, t) \in D := \{(x_1, t) : x_1 \in (-\infty, \infty), \ t \in [0, T]\},$$
$$\tau^1_{23}((x_1, x_2, t) = \tau^2_{23}(x_1, x_2, t), \quad \text{at } x_2 = h_1, \quad (x_1, t) \in D := \{(x_1, t) : x_1 \in (-\infty, \infty), \ t \in [0, T]\}, \tag{9}$$

and

$$v_2(x_1, x_2, t) = v_3(x_1, x_2, t), \quad \text{at } x_2 = h_1 + h_2, \quad (x_1, t) \in D := \{(x_1, t) : x_1 \in (-\infty, \infty), \ t \in [0, T]\},$$
$$\tau^2_{23}(x_1, x_2, t) = \tau^3_{23}(x_1, x_2, t), \quad \text{at } x_2 = h_1 + h_2, \quad (x_1, t) \in D := \{(x_1, t) : x_1 \in (-\infty, \infty), \ t \in [0, T]\}. \tag{10}$$

3. Exact Vibrational Displacements

This section attempts to determine the respective exact vibration displacements in the two coating layers v_1 and v_2, as well as in the nonhomogeneous half space v_3. In light of this, a classical analytical method is adopted to accomplish the set goal.

3.1. Exact Vibrational Displacement in the Coatings

Theorem 1. *The harmonic wave solution for Equation (1) is given by*

$$\begin{cases} u_1(x_2) = A_1 \sinh\left[x_2 \sqrt{k^2 - \frac{\omega^2}{s_1^2} - \frac{\Omega^2}{s_1^2}}\right] + B_1 \cosh\left[x_2 \sqrt{k^2 - \frac{\omega^2}{s_1^2} - \frac{\Omega^2}{s_1^2}}\right], & 0 \leq x_2 \leq h_1, \\\\ u_2(x_2) = A_2 \sinh\left[x_2 \sqrt{k^2 - \frac{\omega^2}{s_2^2} - \frac{\Omega^2}{s_2^2}}\right] + B_2 \cosh\left[x_2 \sqrt{k^2 - \frac{\omega^2}{s_2^2} - \frac{\Omega^2}{s_2^2}}\right], & h_1 \leq x_2 \leq h_1 + h_2, \end{cases} \tag{11}$$

where $A_1, A_2, B_1,$ and B_2 are constants to be determined from the prescribed boundary and interfacial conditions.

Proof. Upon substituting the constitutive equation of the coatings given in Equation (2) into the equations of motions in Equation (1), the following wave-like equations are thus obtained:

$$s_c^2 \left(\frac{\partial^2 v_c}{\partial x_2^2} + \frac{\partial^2 v_c}{\partial x_1^2} \right) = \frac{\partial^2 v_c}{\partial t^2} - \Omega^2 v_c, \qquad c = 1, 2, \tag{12}$$

where s_c for $c = 1, 2$ are the respective shear speeds in the upper and lower coatings, respectively, given by

$$s_c = \sqrt{\frac{\mu_c}{\rho_c}}, \qquad c = 1, 2.$$

What is more, upon deploying the harmonic wave solutions of the following form

$$v_c(x_1, x_2, t) = u_c(x_2) \exp(i(kx_1 - \omega t)), \qquad c = 1, 2, \tag{13}$$

where k and ω are the dimensional wavenumber and frequency, respectively, then Equation (12) reduces to the following ordinary differential models:

$$\frac{d^2 u_c}{dx_2^2} - \left(k^2 - \frac{\omega^2}{s_c^2} - \frac{\Omega^2}{s_c^2} \right) u_c = 0, \qquad c = 1, 2. \tag{14}$$

Finally, Theorem 1 is evident upon solving the above ordinary differential equations layer-wise. □

3.2. Exact Vibrational Displacement in the Nonhomogeneous Half Space

Theorem 2. *The bounded harmonic wave solution for Equation (3) is given by*

$$u_3(x_2) = A_3 \exp\left[-\left(\frac{\beta}{2} + \sqrt{\frac{\beta^2}{4} + k^2 - \frac{\omega^2}{s_3^2} - \frac{\Omega^2}{s_3^2}} \right) x_2 \right]. \tag{15}$$

where A_3 is a constant to be obtained from the prescribed boundary and interfacial conditions.

Proof. By substituting the constitutive equation of the nonhomogeneous half space layer given in Equation (4) into the equation of motion in Equation (3), one obtains the following equation:

$$s_3^2 \left(\frac{\partial^2 v_3}{\partial x_2^2} + \beta \frac{\partial v_3}{\partial x_2} + \frac{\partial^2 v_3}{\partial x_1^2} \right) = \frac{\partial^2 v_3}{\partial t^2} - \Omega^2 v_3, \tag{16}$$

where s_3 is the shear speed in the nonhomogeneous half space given by

$$s_3 = \sqrt{\frac{\mu_3}{\rho_3}},$$

while β is the nonhomogeneity parameter. Thus, upon deploying the harmonic wave solution of the following form

$$v_3(x_1, x_2, t) = u_3(x_2) \exp(i(kx_1 - \omega t)), \tag{17}$$

where k and ω are the dimensional wavenumber and frequency, respectively, then Equation (16) reduces to the following differential equation:

$$\frac{d^2 u_3}{dx_2^2} + \beta \frac{du_3}{dx_2} - \left(k^2 - \frac{\omega^2}{s_3^2} - \frac{\Omega^2}{s_3^2} \right) u_3 = 0. \tag{18}$$

Now, since the layer is semi-infinite, the following solution form is assumed in order to maintain the boundedness of the solution as $x_2 \to \infty$:

$$u_3(x_2) = z(x_2) \exp\left(-\frac{\beta}{2} x_2\right), \tag{19}$$

such that Equation (18) becomes

$$\frac{d^2 z}{dx_2^2} - \left(\frac{\beta^2}{4} + k^2 - \frac{\omega^2}{s_3^2} - \frac{\Omega^2}{s_3^2}\right) z(x_2) = 0, \tag{20}$$

where the later equation has the following solution:

$$z(x_2) = A_3 \exp\left[-x_2 \sqrt{\frac{\beta^2}{4} + k^2 - \frac{\omega^2}{s_3^2} - \frac{\Omega^2}{s_3^2}}\right] + B_3 \exp\left[x_2 \sqrt{\frac{\beta^2}{4} + k^2 - \frac{\omega^2}{s_3^2} - \frac{\Omega^2}{s_3^2}}\right], \tag{21}$$

with A_3 and B_3 as constants to be obtained later on from the prescribed conditions.

Thus, the solution obtained in the above equation as $x_2 \to \infty$ reduces to the following:

$$z(x_2) = A_3 \exp\left[-x_2 \sqrt{\frac{\beta^2}{4} + k^2 - \frac{\omega^2}{s_3^2} - \frac{\Omega^2}{s_3^2}}\right]. \tag{22}$$

Finally, Theorem 2 is evident from Equations (19) and (22). □

4. Exact Dispersion Relation

This section establishes the resulting exact dispersion relations corresponding to both the unloaded and loaded end surface conditions. In doing so, the upper coating layer is further assumed to have a similar shear speed to that of the half-space layer. However, the exponentially varying material constants are only associated with the half space. Therefore, this assumption of $s_1 = s_3$ yields

$$\mu_1 = \mu_3, \qquad \rho_1 = \rho_3. \tag{23}$$

Hence, this development further results in the following basic dimensionless quantities:

$$h = \frac{h_2}{h_1}, \qquad \mu = \frac{\mu_2}{\mu_1}, \qquad \rho = \frac{\rho_2}{\rho_1}, \tag{24}$$

together with

$$K = kh_1, \qquad \chi = \frac{\omega h_1}{s_1}, \qquad \Theta = \frac{\Omega h_1}{s_1}, \qquad \alpha = \beta h_1, \tag{25}$$

where K is the dimensionless wavenumber, χ is the dimensionless frequency, Θ is the dimensionless angular velocity in favour of the rotation, and α is the rescaled nonhomogeneity parameter.

4.1. Exact Dispersion Relation with the Unloaded End Surface Condition

In this case, we make use of the boundary condition associated with the unloaded end surface (traction-free) condition given in Equation (6) together with the perfect interfacial conditions prescribed in Equations (9) and (10) to acquire the resulting dispersion relation. When substituting the aforementioned conditions into the earlier obtained exact solutions of all the three layers under consideration, the dimensionless dispersion matrix is obtained as follows:

$$
D_1 = \begin{pmatrix}
1 & 0 & 0 & 0 & 0 \\
\sinh(\gamma_1) & \cosh(\gamma_1) & -\sinh(\gamma_2) & -\cosh(\gamma_2) & 0 \\
\cosh(\gamma_1)\gamma_1 & \sinh(\gamma_1)\gamma_1 & -\mu\cosh(\gamma_2)\gamma_2 & -\mu\sinh(\gamma_2)\gamma_2 & 0 \\
0 & 0 & \sinh((h+1)\gamma_2) & \cosh((h+1)\gamma_2) & -e^{-(h+1)\gamma_3} \\
0 & 0 & \mu\cosh((h+1)\gamma_2)\gamma_2 & \mu\sinh((h+1)\gamma_2)\gamma_2 & e^{-(h+1)\gamma_3}\gamma_3
\end{pmatrix}, \tag{26}
$$

where γ_j for $j = 1, 2, 3$ appearing in the above equation are dimensionless quantities given by

$$
\gamma_1 = \sqrt{K^2 - \chi^2 - \Theta^2}, \qquad \gamma_2 = \sqrt{K^2 - \frac{\mu}{\rho}\chi^2 - \frac{\mu}{\rho}\Theta^2}, \qquad \gamma_3 = \frac{\alpha}{2} + \sqrt{\frac{\alpha^2}{4} + \gamma_1^2}. \tag{27}
$$

Theorem 3. *The overall exact dispersion relation in the case of the unloaded end surface condition is given as follows:*

$$
\gamma_2^2\,\mu^2\,\tanh(\gamma_2) + \gamma_2\,\mu(\gamma_3 + \gamma_1\,\tanh(\gamma_1 h)) + \gamma_1\,\gamma_3\,\tanh(\gamma_2)\,\tanh(\gamma_1 h) = 0, \tag{28}
$$

where γ_j for $j = 1, 2, 3$ are given in Equation (27).

Proof. The proof follows directly upon setting the resulting determinant of the dispersion matrix expressed in Equation (26) to zero. □

Lemma 1. *A very special case of Theorem 3 is when the nonhomogeneity in the half spaces vanishes (i.e., when $\alpha = 0$). In this case, $\gamma_1 = \gamma_3$ and further yields the following dispersion relation:*

$$
\left(\gamma_2^2\,\mu^2 + \gamma_1^2\,\tanh(\gamma_1 h)\right)\tanh(\gamma_2) + \gamma_1\,\gamma_2\,\mu(1 + \tanh(\gamma_1 h)) = 0. \tag{29}
$$

4.2. Exact Dispersion Relation with the Loaded End Surface Condition

Here, the exact dispersion relation with the loaded end surface condition given in Equation (7) is determined. To be precise, the case of an elastic Winkler foundation given in Equation (8) is analyzed in this subsection. Moreover, a new dimensionless stiffness of the elastic Winkler foundation has been discovered to be ζ, defined as

$$
\zeta = \frac{p\,h_2}{\mu_1}, \tag{30}
$$

where p is the dimensional stiffness of the elastic Winkler foundation.

Therefore, the resulting dispersion matrix in the presence of loaded end surface condition is found to be

$$
D_2 = \begin{pmatrix}
h\gamma_1 & \zeta & 0 & 0 & 0 \\
\sinh(\gamma_1) & \cosh(\gamma_1) & -\sinh(\gamma_2) & -\cosh(\gamma_2) & 0 \\
\cosh(\gamma_1)\gamma_1 & \sinh(\gamma_1)\gamma_1 & -\mu\cosh(\gamma_2)\gamma_2 & -\mu\sinh(\gamma_2)\gamma_2 & 0 \\
0 & 0 & \sinh((h+1)\gamma_2) & \cosh((h+1)\gamma_2) & -e^{-(h+1)\gamma_3} \\
0 & 0 & \mu\cosh((h+1)\gamma_2)\gamma_2 & \mu\sinh((h+1)\gamma_2)\gamma_2 & e^{-(h+1)\gamma_3}\gamma_3
\end{pmatrix}. \tag{31}
$$

Theorem 4. *The overall exact dispersion relation in the case of the loaded end surface condition is given as follows:*

$$
\left(\gamma_2^2\mu^2\tanh(\gamma_2) + \gamma_2\mu(\gamma_3 + \gamma_1\tanh(\gamma_1 h)) + \gamma_1\gamma_3\tanh(\gamma_2)\tanh(\gamma_1 h)\right) -
$$
$$
\frac{\zeta}{\gamma_1 h}(\gamma_1(\gamma_2\mu + \gamma_3\tanh(\gamma_2)) + \gamma_2\mu(\gamma_2\mu\tanh(\gamma_2) + \gamma_3)\tanh(\gamma_1 h)) = 0, \tag{32}
$$

where γ_j for $j = 1, 2, 3$ are given in Equation (27).

Similarly, the proof of Theorem 4 follows as in Theorem 3 via setting the dispersion relation expressed in Equation (31) to zero.

Lemma 2. *Theorem 4 reduces to Theorem 3 upon setting $\zeta = 0$.*

Lemma 3. *A very special case of Theorem 4 is when the nonhomogeneity in the half spaces vanishes (i.e., when $\alpha = 0$). In this case, $\gamma_1 = \gamma_3$ and further yields the following dispersion relation:*

$$
\gamma_2^2 \mu^2 \tanh(\gamma_2) + \gamma_2 \mu (\gamma_1 + \gamma_1 \tanh(\gamma_1 h)) + \gamma_1^2 \tanh(\gamma_2) \tanh(\gamma_1 h) -
$$
$$
\frac{\zeta}{\gamma_1 h} (\gamma_1 (\gamma_2 \mu + \gamma_1 \tanh(\gamma_2)) + \gamma_2 \mu (\gamma_2 \mu \tanh(\gamma_2) + \gamma_1) \tanh(\gamma_1 h)) = 0.
$$

(33)

Additionally, as the propagation with a long wave and low frequency is attained at $K \ll 1$, and $\chi \ll 1$, we therefore quote the following statement as a remark in connection to the obtained respective dispersion relations:

Remark 1. *"The transcendental dispersion relation allows polynomial asymptotic expansions at the long-wave limit $K \ll 1$" [15].*

Moreover, a similar remark can be drawn upon with regard to the low frequency limit $\chi \ll 1$.

5. Approximation

This section establishes approximate dispersion relations corresponding to both the unloaded and loaded end surface conditions via the application of an asymptotic approximation procedure. To accomplish this, certain effective boundary conditions will be derived and thereafter utilized to approximate the governing equations of motions such that they lead to the optimal approximate dispersion relations.

5.1. Effective Boundary Conditions

To derive the appropriate effective boundary conditions, it is convenient to set the following boundary conditions at the interfaces such that

$$
\begin{aligned}
v_1 = w_1 \quad &\text{at} \quad x_2 = h_1, \\
v_2 = w_2 \quad &\text{at} \quad x_2 = h_1 + h_2,
\end{aligned}
$$

(34)

where $w_c = w_c(x_1, x_2, t)$, for $c = 1, 2$ are certain prescribed displacements.

5.1.1. Procedure for the Upper Coating Layer $(c = 1)$

We reduce the effect of the upper coating layer by means of effective boundary conditions. To begin with, let us specify a small parameter ε in the long wave limit as

$$
\varepsilon = \frac{h_1 + h_2}{L} \ll 1, \quad \left(k \sim \frac{1}{L} \right),
$$

(35)

where L is a typical wave length. In addition, we introduce the following scaling:

$$
\xi_l = \frac{x_1}{L}, \qquad \eta_1 = \frac{x_2 + h_2}{h_1 + h_2}, \qquad \tau_c = \frac{s_c t}{L},
$$

(36)

along with

$$
v_c^* = \frac{v_c}{L}, \quad w_c^* = \frac{w_c}{L}, \quad \tau_{13}^{(*,c)} = \frac{\tau_{13}^c}{\mu_c}, \quad \tau_{23}^{(*,c)} = \frac{\tau_{23}^c}{\varepsilon \mu_c}, \quad p_c^* = \frac{p L}{\varepsilon \mu_c}, \quad \Omega_c^* = \frac{\Omega L}{s_c},
$$

(37)

where $c = 1, 2$ and all quantities with an asterisk are assumed to have the same asymptotic order.

Therefore, the equation of motion given in Equation (1) and the constitutive relations in Equation (2) are rewritten for $c = 1$ as

$$\frac{\partial \tau_{23}^{(*,1)}}{\partial \eta_1} + \frac{\partial \tau_{13}^{(*,1)}}{\partial \xi_l} = \frac{\partial^2 v_1^*}{\partial \tau_1^2} - \Omega_1^{*2} v_1^*, \quad \tau_{13}^{(*,1)} = \frac{\partial v_1^*}{\partial \xi_l}, \quad \varepsilon^2 \tau_{23}^{(*,1)} = \frac{\partial v_1^*}{\partial \eta_1}, \tag{38}$$

where the boundary conditions given in Equations (7) and $(34)_1$ become

$$\tau_{23}^{(*,1)} = -p_1^* v_1^* \quad \text{at} \quad \eta_1 = \theta_2, \quad \text{and} \quad v_1^* = w_1^* \quad \text{at} \quad \eta_1 = 1, \tag{39}$$

with $\theta_2 = h_2/(h_1 + h_2)$.

Moreover, we expand the involved displacements and stresses via asymptotic series as follows:

$$\begin{pmatrix} v_c^* \\ \tau_{13}^{(*,c)} \\ \tau_{23}^{(*,c)} \end{pmatrix} = \begin{pmatrix} v_c^{(0)} \\ \tau_{13}^{(0,c)} \\ \tau_{23}^{(0,c)} \end{pmatrix} + \varepsilon \dots, \tag{40}$$

Then, at the leading order, Equation (38) becomes

$$\frac{\partial \tau_{23}^{(0,1)}}{\partial \eta_1} + \frac{\partial \tau_{13}^{(0,1)}}{\partial \xi_l} = \frac{\partial^2 v_1^{(0)}}{\partial \tau_1^2} - \Omega_1^{*2} v_1^{(0)}, \quad \tau_{13}^{(0,1)} = \frac{\partial v_1^{(0)}}{\partial \xi_l}, \quad \frac{\partial v_1^{(0)}}{\partial \eta_1} = 0, \tag{41}$$

while the boundary conditions determined in Equation (39) become

$$\tau_{23}^{(0,1)} = -p_1^* v_1^{(0)} \quad \text{at} \quad \eta_1 = \theta_2, \quad \text{and} \quad v_1^{(0)} = w_1^* \quad \text{at} \quad \eta_1 = 1, \tag{42}$$

Hence, the solution of the above system is obtained as follows:

$$v_1^{(0)} = w_1^*, \quad \tau_{13}^{(0,1)} = \frac{\partial w_1^*}{\partial \xi_l}, \quad \tau_{23}^{(0,1)} = (\eta_1 - \theta_2)\left(\frac{\partial^2 w_1^*}{\partial \tau_1^2} - \frac{\partial^2 w_1^*}{\partial \xi_l^2} - \Omega_1^{*2} w_1^*\right) - p_1^* w_1^*. \tag{43}$$

Moreover, upon returning to the original variables, the effective boundary conditions at the interface $x_2 = h_1$ may be obtained as follows:

$$\tau_{23}^2 = h_1 \left(\rho_1 \left(\frac{\partial^2 v_2}{\partial t^2} - \Omega^2 v_2 \right) - \mu_1 \frac{\partial^2 v_2}{\partial x_1^2} \right) - p v_2. \tag{44}$$

5.1.2. Procedure for the Lower Coating Layer ($c = 2$)

Now, let us perform a similar treatment for the lower coating layer by first adopting the following quantity:

$$\eta_2 = \frac{x_2}{h_1 + h_2}, \tag{45}$$

We adopt this along with the dimensionless quantities defined earlier in Equations (36) and (37). Moreover, the equations of motion given in Equation (1) and the constitutive relations given in Equation (2) at $c = 2$ can be reformed in the new variables as

$$\frac{\partial \tau_{23}^{(*,2)}}{\partial \eta_2} + \frac{\partial \tau_{13}^{(*,2)}}{\partial \xi_l} = \frac{\partial^2 v_2^*}{\partial \tau^2} - \Omega_2^{*2} v_2^*, \quad \tau_{13}^{(*,2)} = \frac{\partial v_2^*}{\partial \xi_l}, \quad \varepsilon^2 \tau_{23}^{(*,2)} = \frac{\partial v_2^*}{\partial \eta_2}, \tag{46}$$

subject to the boundary conditions

$$\tau_{23}^{(*,2)} = \theta_1\left(\frac{\rho_1}{\rho_2}\left(\frac{\partial^2 v_2^*}{\partial \tau_2^2} - \Omega^{*2}\, v_2^*\right) - \frac{\mu_1}{\mu_2}\frac{\partial^2 v_2^*}{\partial \xi_l^2}\right) - p_2^* v_2^* \qquad \text{at} \qquad \eta_2 = \theta_1,$$

$$\text{and} \quad v_2^* = w_2^* \qquad \text{at} \qquad \eta_2 = 1, \tag{47}$$

where $\theta_1 = h_1/(h_1 + h_2)$.

Therefore, at the leading order $O(1)$, we have

$$\frac{\partial \tau_{23}^{(0,2)}}{\partial \eta_2} + \frac{\partial \tau_{13}^{(0,2)}}{\partial \xi_l} = \frac{\partial^2 v_2^{(0)}}{\partial \tau_2^2} - \Omega_2^{*2}\, v_2^{(0)}, \quad \tau_{13}^{(*,2)} = \frac{\partial v_2^{(0)}}{\partial \xi_l}, \quad \frac{\partial v_2^{(0)}}{\partial \eta_2} = 0, \tag{48}$$

subject to the boundary conditions

$$\tau_{23}^{(0,2)} = \theta_1\left(\frac{\rho_1}{\rho_2}\left(\frac{\partial^2 v_2^{(0)}}{\partial \tau_2^2} - \Omega^{*2}\, v_2^{(0)}\right) - \frac{\mu_1}{\mu_2}\frac{\partial^2 v_2^{(0)}}{\partial \xi_l^2}\right) - p_2^* v_2^{(0)} \qquad \text{at} \qquad \eta_2 = \theta_1,$$

$$\text{and} \quad v_2^{(0)} = w_2^* \qquad \text{at} \qquad \eta_2 = 1. \tag{49}$$

Once again, the solution of the above system yields

$$v_2^{(0)} = w_2^*, \qquad \tau_{13}^{(0,2)} = \frac{\partial w_2^*}{\partial \xi_l}, \tag{50}$$

$$\tau_{23}^{(0,2)} = \left(\eta_2 + \theta_1\left(\frac{\rho_1}{\rho_2} - 1\right)\right)\left(\frac{\partial^2 w_2^*}{\partial \tau_2^2} - \Omega_2^{*2} w_2^*\right) - \left(\eta_2 + \theta_1\left(\frac{\mu_1}{\mu_2} - 1\right)\right)\frac{\partial^2 w_2^*}{\partial \xi_l^2} - p_2^* w_2^*, \tag{51}$$

such that upon returning to the original dimensional variables, the stress determined in Equation (51) at $x_2 = h_1 + h_2$ becomes

$$\tau_{23}^3 = (h_1\,\rho_1 + h_2\,\rho_2)\left(\frac{\partial^2 v_3}{\partial t^2} - \Omega^2\, v_3\right) - (h_1\,\mu_1 + h_2\,\mu_2)\frac{\partial^2 v_3}{\partial x_1^2} - pv_3. \tag{52}$$

5.2. Approximate Dispersion Relation

Having successfully derived the approximate or rather asymptotic expressions for the respective stresses in the upper and lower coating layers, we now aim to determine the approximate dispersion relation with loaded and unloaded end surface conditions in what follows.

Now, having determined the approximate boundary condition in Equation (52), an approximate equation of motion in the presence of a loaded end surface condition is thus constructed as follows

$$\mu_3\, e^{\beta(h_1+h_2)}\frac{\partial v_3}{\partial x_2} - (h_1\,\rho_1 + h_2\,\rho_2)\left(\frac{\partial^2 v_3}{\partial t^2} - \Omega^2\, v_3\right) + (h_1\,\mu_1 + h_2\,\mu_2)\frac{\partial^2 v_3}{\partial x_1^2} = -pv_3. \tag{53}$$

Thus, the main results of the present Section are contained in what follows:

Theorem 5. *The approximate dispersion relation in the case of the loaded end surface condition is given by*

$$\gamma_3\, e^{\alpha(h+1)} + K^2(1 + h\mu) - (1 + h\rho)\left(\chi^2 + \Theta^2\right) - \frac{\zeta}{h} = 0. \tag{54}$$

Proof. Without a loss of generality, the present proof follows upon applying Equations (17) and (15) into Equation (53). □

Lemma 4. *The approximate dispersion relation with the unloaded end surface condition follows from Theorem 5 when ζ = 0 as follows*

$$\gamma_3\, e^{\alpha(h+1)} + K^2(1+h\mu) - (1+h\rho)\left(\chi^2 + \Theta^2\right) = 0. \tag{55}$$

Thus, we have shown in what follows the comparison between the exact and approximate dispersion relations with a loaded end surface condition determined in Equations (54) and (32), respectively, in Figure 2, while the comparison between the exact and approximate dispersion curves with an unloaded end surface condition determined in Equations (55) and (28), respectively, is depicted in Figure 3. Importantly, these figures showed perfect agreement between the exact and approximate fundamental modes in both cases. In addition, the case of a soft elastic Winkler foundation was considered by setting ζ = 0.01 in Figure 3, as was asserted by Erbas et al. [43].
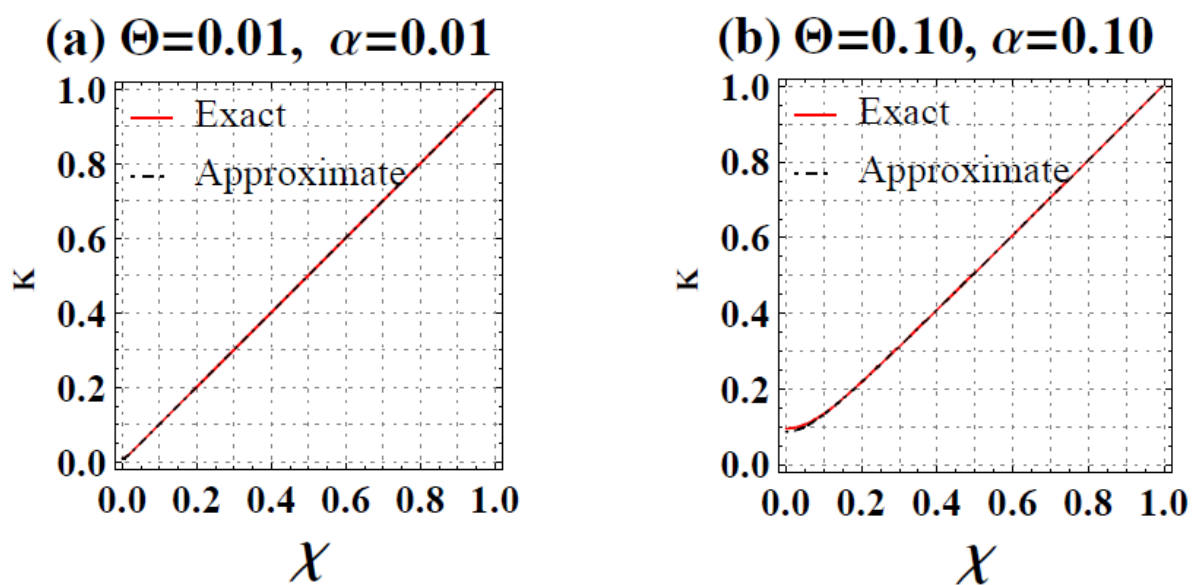

Figure 2. Comparison between the exact and asymptotic fundamental modes with an unloaded end surface condition.
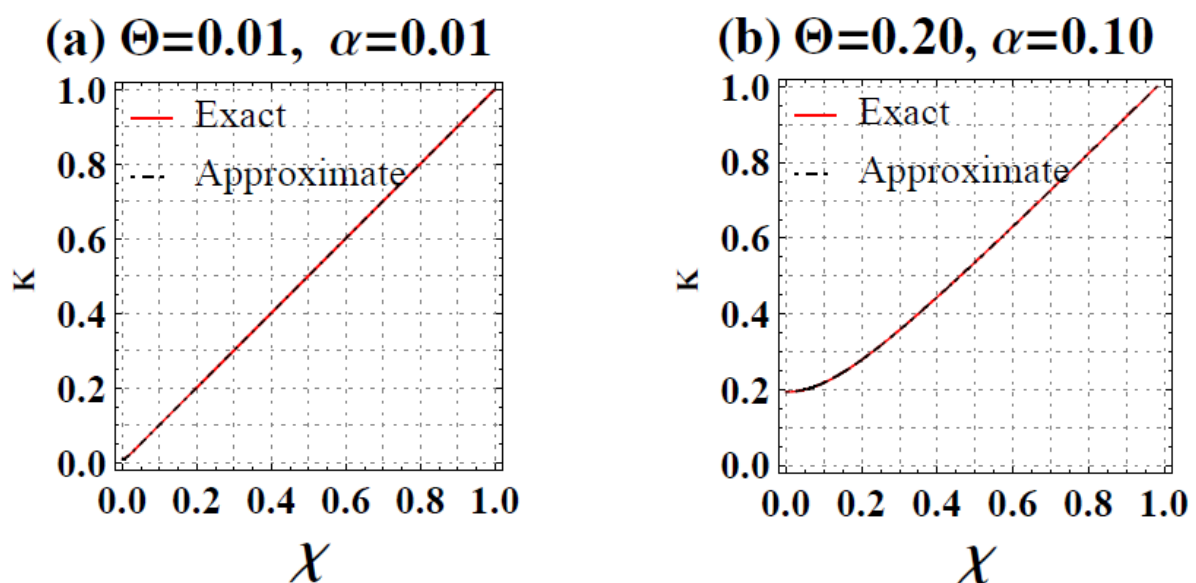

Figure 3. Comparison between the exact and asymptotic fundamental modes with a loaded end surface condition when ζ = 0.01.

6. Application and Discussion of Results

More recently, Mandi et al. [38] examined the case of propagating Love waves in a double-layered structure resting over inhomogeneous semi-infinite media. As an application, the double-layered structure was considered to be made of a combination of a fiber-reinforced medium and a dry sandy medium while perfectly resting over inhomogeneous semi-infinite media. However, having made the assumption of alternating layers with non-dimensionalization for the present obtained dispersion relations and, at the same time, not forgetting the presence of the material nonhomogeneity in the half space, we therefore, for the sake of numerical simulation, considered the physical data reported in [38] by considering an arbitrary material in the upper coating layer, a dry sandy lower coating, and the same arbitrary material in the half space in the presence of nonhomogeneity α. These data are tabulated in Table 1.

Table 1. Material constants in the respective regions of the structure [38].

Layer	Lame's Constant ($\times 10^{10}$ Nm^{-2})	Density ($\times 10^3$ kgm^{-3})	Thickness (m)
Upper coating	$\mu_1 = 7.10$	$\rho_1 = 3.32$	$h_1 = 1.00$
Lower coating (dry sandy)	$\mu_2 = 6.54$	$\rho_2 = 3.40$	$h_2 = 0.50$
Nonhomogeneous half space	$\mu_3 = 7.10$	$\rho_3 = 3.32$	Semi-infinite

Furthermore, we studied the variational effects of the material nonhomogeneity in cases of unloaded and loaded end surface conditions, while the effect of the elastic Winkler foundation was examined specifically with regard to the loaded scenario. Thus, Figure 4 portrays the variation of the fundamental mode with respect to the variation of the nonhomogeneity parameter α at various fixed angular velocities Θ, while Figures 5 and 6 show the corresponding plots with regard to the loaded end surface condition and with respect to the variation of the nonhomogeneity parameter α and the elastic Winkler foundation parameter ζ, respectively.
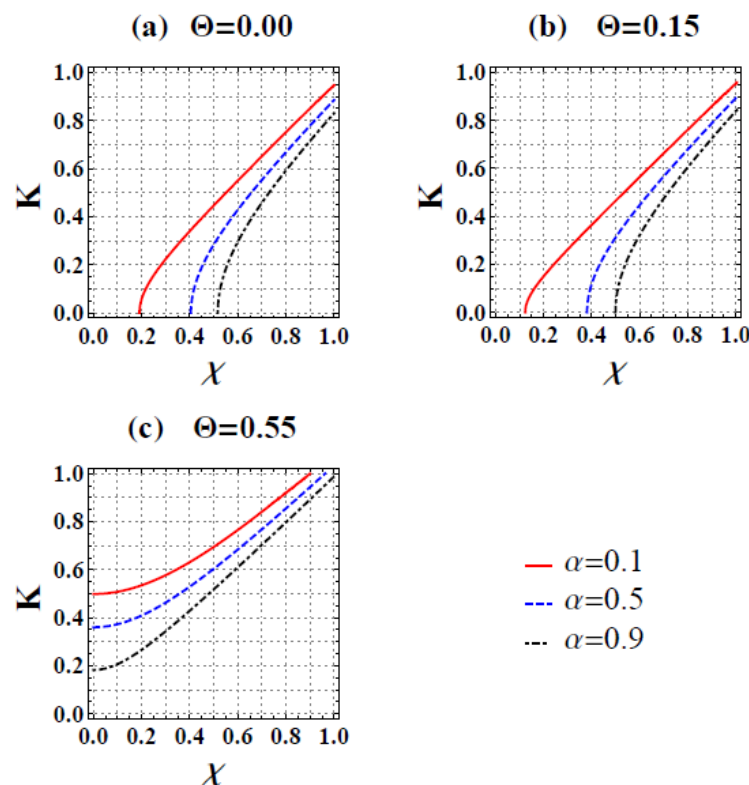

Figure 4. Response of the fundamental mode to the variation of the nonhomogeneity parameter α at a different fixed angular velocity Θ (unloaded end surface case).

Before discussing these figures, it would be relevant to mention here that the presence of the nonhomogeneity parameter α and the rotation presided over by the angular velocity Θ were what prevented the fundamental mode to start propagating from zero $(0,0)$. Clear evidence of this can be seen in Figures 2a and 3a, where these parameters were taken to be negligible. Hence, Figure 4 portrays the variation of the fundamental mode with respect to the variation of the nonhomogeneity parameter α at various fixed angular velocities Θ. Evidently, in the absence of the angular velocity $\Theta = 0$, as shown in Figure 4a, an increase in the nonhomogeneity parameter α resulted in propagation with a relatively long frequency. This was due to the fact that the fundamental mode was continuously moving toward $\chi = 1$, and the fact that low-frequency propagation always satisfies the condition $\chi \ll 1$ [16–19]. Moreover, the same trend was applied to Figure 4b, except that the propagation at $\alpha = 0.1$ had a wider validity range of low frequencies. Additionally, the case of the higher value of the angular velocity, as in Figure 4c, was a completely different one. In fact, the fundamental mode curves were over the wavenumber axis K, with the highest nonhomogeneity parameter value $\alpha = 0.9$ having a wider long-wave validity range.

Moreover, the same interpretation of Figure 4 applies to Figure 5 for the case of the loaded end surface condition. However, one could observe the effect of the presence of a soft elastic Winkler foundation when $\zeta = 0.01$. To be precise, the presence of an elastic foundation proliferated the transition between having a fundamental mode over the χ-axis to the K-axis as the angular velocity increased.

This interpretation would equally be extended to the case of Figure 6 where, in this case, the variational effect of an elastic Winkler foundation parameter ζ is portrayed. According to Figure 6a, when $\Theta = 0$, one can observe that the fundamental mode had the widest validity range over a long-wave interval when $\zeta = 0.01$, and gradually shrank as ζ increased. Additionally, this was due to the fact that we considered a soft foundation (i.e., $\zeta \ll 1$) [43]. Moreover, the same interpretation was applied to Figure 6b,c, except that an increase in the angular velocity Θ reduced the vicinity of the long-wave range.
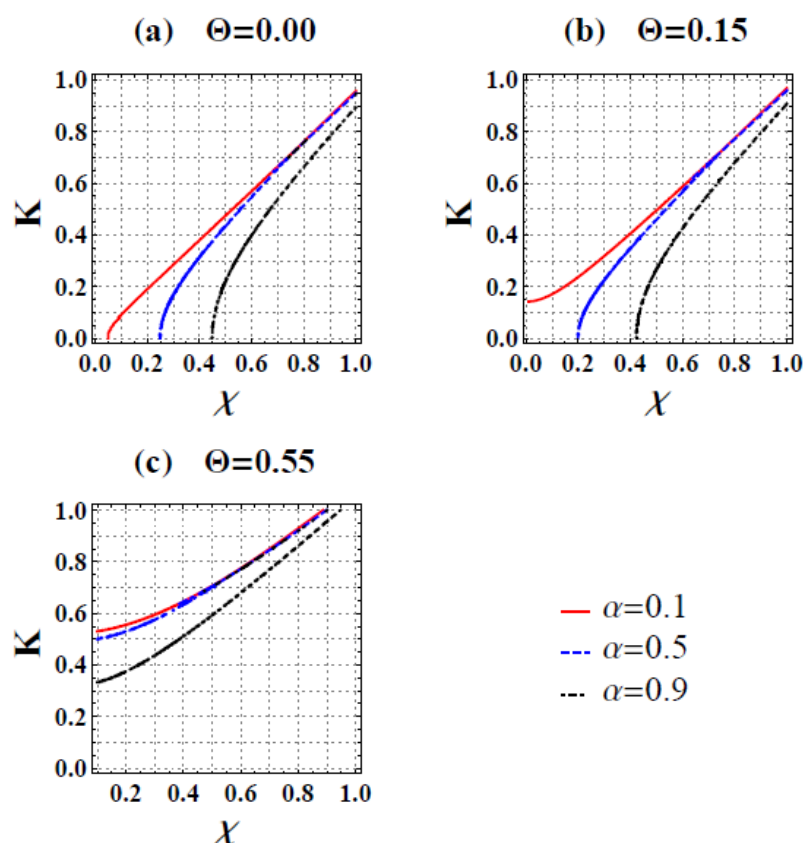

Figure 5. Response of the fundamental mode to the variation of the nonhomogeneity parameter α at a different fixed angular velocity Θ when $\zeta = 0.01$ (loaded end surface case).

(a) Θ=0.00

(b) Θ=0.15

(c) Θ=0.55

— $\zeta=0.01$
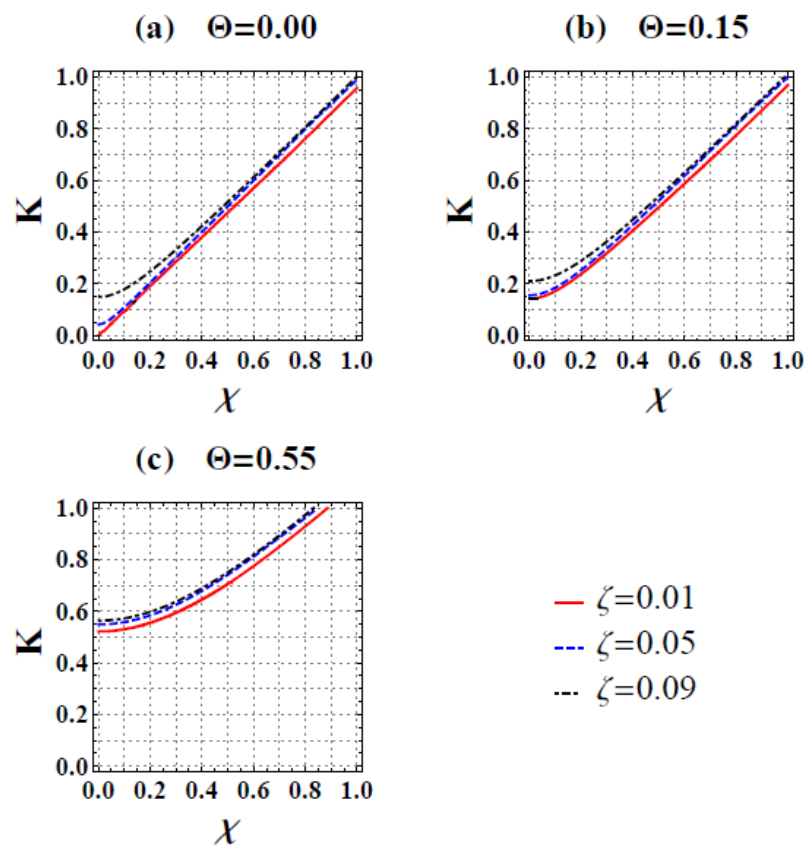--- $\zeta=0.05$
--- $\zeta=0.09$

Figure 6. Response of the fundamental mode to the variation of soft elastic Winkler foundation parameter ζ at a different fixed angular velocity Θ when $\alpha = 0.1$ (loaded end surface case).

7. Conclusions

In conclusion, the current manuscript examined the propagation of surface waves in a rotating, doubly coated nonhomogeneous half space. The coating layers were assumed to be made of different homogeneous isotropic materials, while that of the half space was of a nonhomogeneous material. Perfect bonding conditions were prescribed between the layers, in addition to the prescription of two end surface conditions on the outer layer. An analytical approach was employed for the determination of the consequential exact vibrational displacements and dispersion relation, in addition to the deployment of an asymptotic approximation method for the validation of the obtained analytical results within the long-wave limit. Two cases of mechanically unloaded and loaded end surface scenarios were analyzed through their respective fundamental modes. Moreover, an elastic Winkler foundation was considered in the case of the mechanically loaded end surface condition. More precisely, the presence of an elastic foundation was found to proliferate the transition between having a fundamental mode over the dimensionless frequency axis to the axis of the dimensionless wavenumber as the angular velocity increased. In addition, smaller values for the angular velocity were found to ensure a propagation with a low frequency, while long-wave propagation was ensured through higher values for the angular velocity. Aside from that, an increase in the nonhomogeneity parameter α was discovered to result in propagation with a relatively long frequency. This was due to the fact that the fundamental mode was continuously moving toward $\chi = 1$. Finally, the present study can be extended to the case of multi-coat half spaces in the presence of, for example, an external influence.

References

1. Achenbach, J.D. *Wave Propagation in Elastic Solids, Eight Impression*; Elsevier: Amsterdam, The Netherlands, 1999.
2. Alzaidi, A.S.M.; Mubaraki, A.M.; Nuruddeen, R.I. Effect of fractional temporal variation on the vibration of waves on elastic substrates with spatial non-homogeneity. *AIMS Math.* 2022, *accepted*.
3. Andrianov, I.V.; Awrejcewicz, J.; Danishevs'kyy, V.V.; Ivankov, O.A. *Asymtotic Methods in the Theory of Plates with Mixed Boundary Conditions*; John Wiley & Sons, Ltd.: Hoboken, NJ, USA, 2014.
4. Ewing, W.M.; Jardetzky, W.S.; Press, F.; Beiser, A. Elastic Waves in Layered Media. *Phys. Today* **1957**, *10*. [CrossRef]
5. Daniel, I.M.; Ishai, O.; Daniel, I.M.; Daniel, I. *Engineering Mechanics of Composite Materials*; Oxford University Press: New York, NY, USA, 2006.
6. Vinson, J. *The Behavior of Sandwich Structures of Isotropic and Composite Materials*; Routledge: London, UK, 2018.
7. Green, W. Bending waves in strongly anisotropic elastic plates. *Q. J. Mech. Appl. Math.* **1982**, *35*, 485–507. [CrossRef]
8. Kaplunov, J.; Nobili, A. Multi-parametric analysis of strongly inhomogeneous periodic waveguides with internal cutoff frequencies. *Math. Methods Appl. Sci.* **2017**, *40*, 3381–3392. [CrossRef]
9. Nuruddeen, R.I.; Nawaz, R.; Zia, Q.M.Z. Investigating the viscous damping effects on the propagation of Rayleigh waves in a three-layered inhomogeneous plate. *Phys. Scr.* **2020**, *95*, 065224. [CrossRef]
10. Abd-Alla, A.M.; Abo-Dahab, S.M.; Khan, A. Rotational effects on magneto-thermoelastic Stoneley, Love, and Rayleigh waves in fibre-reinforced anisotropic general viscoelastic media of higher order. *Comput. Mater. Contin.* **2017**, *53*, 49–72.
11. Abo-Dahab, S.M.; Lotfy, K.; Gohaly, K.A. Rotation and magnetic field effect on surface waves propagation in an elastic layer lying over a generalized thermoelastic diffusive half-space with imperfect boundary. *Math. Probl. Eng.* **2015**, *2015*, 671783. [CrossRef]
12. Nuruddeen, R.I.; Nawaz, R.; Zia, Z.Q.M. Effects of thermal stress, magnetic field and rotation on the dispersion of elastic waves in an inhomogeneous five-layered plate with alternating components. *Sci. Prog.* **2020**, *103*, 0036850420940469. [CrossRef]
13. Kaplunov, J.; Prikazchikov, D.A.; Prikazchikov, L.A.; Sergushova, O. The lowest vibration spectra of multi-component structures with contrast material properties. *J. Sound Vib.* **2019**, *445*, 132–147. [CrossRef]
14. Wang, Y.Z.; Li, M.F.; Kishimoto, K. Thermal effects on vibration properties of double-layered nanoplates at small scales. *Compos. Part B Eng.* **2011**, *42*, 1311–1317. [CrossRef]
15. Althobaiti, S.; Mubaraki, A.; Nuruddeen, R.I.; Gomez-Aguilar, J.F. Wave propagation in an elastic coaxial hollow cylinder when exposed to thermal heating and external load. *Results Phys.* **2022**. [CrossRef]
16. Kaplunov, J.; Prikazchikov, D.; Prikazchikova, L. Dispersion of elastic waves in a strongly inhomogeneous three-layered plate. *Int. J. Solids Struct.* **2017**, *113*, 169–179. [CrossRef]
17. Nuruddeen, R.; Nawaz, R.; Zia, Q.Z. Asymptotic approach to anti-plane dynamic problem of asymetric three-layered composite plate. *Math. Methods Appl. Sci.* **2021**, *44*, 10933–10947. [CrossRef]
18. Kaplunov, J.; Prikazchikova, L.; Alkinidri, M. Antiplane shear of an asymmetric sandwich plate. *Contin. Mech. Thermodyn.* **2021**, *33*, 1247–1262. [CrossRef]
19. Prikazchikova, L.; Aydn, Y.E.; Erbas, B.; Kaplunov, J. Asymptotic analysis of an anti-plane dynamic problem for a three-layered strongly inhomogeneous laminate. *Math. Mech. Solids* **2020**, *25*, 3–16. [CrossRef]
20. Nuruddeen, R.I.; Nawaz, R.; Zia, Q.Z. Asymptotic analysis of an anti-plane shear dispersion of an elastic five-layered structure amidst contrasting propertie. *Arch. Appl. Mech.* **2020**, *90*, 1875–1892. [CrossRef]
21. Kaplunov, J.D.; Kossovitch, L.Y.; Nolde, E.V. *Dynamics of Thin Walled Elastic Bodies*; Academic Press: Cambridge, MA, USA, 1998.
22. Dai, H.-H.; Kaplunov, J.; Prikachikov, D.A. Long-wave model for the surface wave in a coated half-space. *Proc. R. Soc. A Math. Phys. Eng. Sci.* **2010**. [CrossRef]
23. Vinh, P.C.; Linh, N.T.K. An approximate secular equation of Rayleigh waves propagating in an orthotropic elastic half-space coated by a thin orthotropic elastic layer. *Wave Motion* **2012**, *49*, 681–689. [CrossRef]
24. Vinh, P.C.; Anh, V.T.N.; Thanh, V.P. Rayleigh waves in an isotropic elastic half-space coated by a thin isotropic elastic layer with smooth contact. *Wave Motion* **2014**, *51*, 496–504. [CrossRef]
25. Padture, N.P.; Gell, M.; Jordan, E.H. Thermal barrier coatings for gas-turbine engine application. *Science* **2002**, *296*, 280–284. [CrossRef]

26. Palermo, A.; Krodel, S.; Marzani, A.; Daraio, C. Engineered metabarrier as shield from seismic surface waves. *Sci. Rep.* **2016**, *6*, 39356. [CrossRef] [PubMed]

27. Cho, Y.S. Non-destructive testing of high strength concrete using spectral analysis of surface waves. *NDT Int.* **2003**, *36*, 229–235. [CrossRef]

28. Krylov, V.V. *Noise and Vibration from High-Speed Trains*; Thomas Telford: London, UK, 2001.

29. Tiainen, V.M. Amorphous carbon as a bio-mechanical coating-mechanical properties and biological applications. *Diam. Relat. Mater.* **2001**, *10*, 153–160. [CrossRef]

30. Li, M.; Liu, Q.; Jia, Z.; Xu, X.; Cheng, Y.; Zheng, Y.; Xi, T.; Wei, S. Graphene oxide/hydroxyapatite composite coatings fabricated by electrophoretic nanotechnology for biological applications. *Carbon* **2014**, *67*, 185–197. [CrossRef]

31. Mubaraki, A.; Althobaiti, S.; Nuruddeen, R.I. Propagation of surface waves in a rotating coated viscoelastic half-space under the influence of magnetic field and gravitational forces. *Fractal Fract.* **2021**, *5*, 250. [CrossRef]

32. Mubariki, A.; Prikazchikov, D. On Rayleigh wave field induced by surface stresses under the effect of gravity. *Math. Mech. Solids* **2020**. [CrossRef]

33. Mubaraki, A. Asymptotic Models for Surface Waves in Coated Elastic Solids. Ph.D. Thesis, Keel University, Keele, UK, 2021.

34. Ahmad, F.; Zaman, F.D. Exact and asymptotic solutions of the elastic wave propagation problem in a rod. *Int. J. Pure Appl. Math.* **2006**, *27*, 123–127.

35. Yigit, G.; Sahin, A.; Bayram, M. Modelling of vibration for functionally graded beams. *Open Math.* **2016**, *14*, 661–671. [CrossRef]

36. Horgan, C.; Miller, K. Antiplane shear deformations for homogeneous and inhomogeneous anisotropic linearly elastic solids. *J. Appl. Mech. Mar.* **1994**, *61*, 23–29. [CrossRef]

37. Horgan, C.O. Anti-plane shear deformations in linear and nonlinear solid mechanics. *SIAM Rev.* **1995**, *37*, 53–81. [CrossRef]

38. Mandi, A.; Kundu, S.; Chandra, P.; Pati, P. An analytic study on the dispersion of Love wave propagation in double layers lying over inhomogeneous half-space. *J. Solid Mech.* **2019**, *11*, 570–580.

39. Pal, P.K.; Acharya, D. Effect of inhomogeneity on surface waves in anisotropic media. *Sadhana* **1998**, *23*, 247–258. [CrossRef]

40. Kundu, S.; Kumari, A. Torsional wave propagation in an initially stressed anisotropic heterogeneous crustal layer lying over a viscoelastic half-space. *Procedia Eng.* **2017**, *173*, 980–987. [CrossRef]

41. Alam, P.; Kundu, S. Influences of heterogeneities and initial stresses on the propagation of love-type waves in a transversely isotropic layer over an inhomogeneous half-space. *J. Solid Mech.* **2017**, *9*, 783–793.

42. Shekhar, S.; Parvez, I.A. Propagation of torsional surface waves in an inhomogeneous anisotropic fluid saturated porous layered half space under initial stress with varying properties. *Appl. Math. Model.* **2016**, *40*, 1300–1314. [CrossRef]

43. Erbas, B.; Kaplunov, J.; Nobili, A.; Kilic, G. Dispersion of elastic waves in a layer interacting with a Winkler foundation. *J. Acoust Soc. Am.* **2018**, *144*, 2918–2925. [CrossRef]